INSTITUTE OF PHYSICS PUBLISHING and INTERNATIONAL ATOMIC ENERGY AGENCY NUCLEAR FUSION

Nucl. Fusion **45** (2005) 1446–1450 doi:10.1088/0029-5515/45/11/027

Observation of high-frequency waves during strong tearing mode activity in FTU plasmas without fast ions

P. Buratti, P. Smeulders, F. Zonca, S.V. Annibaldi, M. De Benedetti, H. Kroegler, G. Regnoli, O. Tudisco and the FTU-team

EURATOM-ENEA Association, C.R. Frascati, CP 65, 00044 Frascati, Italy

E-mail: buratti@frascati.enea.it

Received 9 December 2004, accepted for publication 24 August 2005
Published 27 October 2005
Online at stacks.iop.org/NF/45/1446

Abstract

MHD spectroscopy in FTU has revealed high frequency (HF) oscillations between 30 and 70 kHz that accompany the development of large $m_0 = -2$, $n_0 = -1$ islands in ohmic plasmas. This frequency range is one order of magnitude above the island rotation frequency, one order of magnitude below the first toroidal gap in the Alfvén continuum and of the same order of the low frequency gap introduced by finite beta effects. The HF spectrum is organized in pairs of modes with opposite toroidal numbers, $n = 1$ and $n = -1$ for the stronger ones, which form standing waves in the island rest frame. The poloidal structure of HF modes is $|m| = 2$ for the main lines. HF lines appear when the level of poloidal field perturbation produced by the island at the plasma edge exceeds 0.2%. The absence of energetic ions in FTU ohmic plasmas, the strict correlation between HF and tearing modes and the existence of a threshold indicate that HF modes tap their energy from the tearing mode by a non-linear coupling mechanism.

PACS numbers: 52.35.Bj, 52.35.Py

1. Introduction

High frequency (HF) oscillations in magnetically confined plasmas have been identified as discrete Alfvén eigenmodes (AEs) excited by high-energy ions [1]. Frequencies of discrete AE stay in gaps that are introduced in the shear-Alfvén continuum by poloidal mode coupling due to toroidicity, ellipticity and other equilibrium features. AE typically have much larger frequencies than other plasma instabilities such as tearing modes or fishbones. The frequency of toroidicity-induced Alfvén eigenmodes (TAEs) is $\omega_{\mathrm{TAE}} = \omega_{\mathrm{A}}/2 = V_{\mathrm{A}}/(2qR_0)$, where V_{A}, q and R_0 are the Alfvén velocity, safety factor and major radius, respectively. Other gaps introduced by equilibrium features have even higher frequencies. Energetic ion losses due to Alfvén waves at frequencies below ω_{TAE} have been found in some experiments [2]. These waves have been named beta-induced Alfvén eigenmodes (BAEs) since their frequency is located in a gap $0 < (\omega/\omega_{\mathrm{A}})^2 < \gamma\beta q^2$ [1], which is caused by finite plasma compressibility. Here γ is the ratio of specific heats and β the ratio of kinetic and magnetic pressures. While experimental evidence of BAE modes was originally due to the circulating fast ion population [2], the main effect of such fluctuations in a burning plasma will be from trapped alpha particles due to their low frequency [3, 4]. The low frequency shear Alfvén gap also appears to be the explanation of the low frequency feature of Alfvén cascades in JET [5].

MHD spectroscopy measurements in FTU have revealed the existence of HF waves in ohmic plasmas, i.e. in plasmas without any fast ion population. HF waves appear as a multiplicity of lines between 30 and 70 kHz (figure 1), whereas the oscillation frequencies associated with tearing modes is typically below 5 kHz, with weaker harmonics extending up to 20 kHz. The frequency range of HF waves is of the same order of the gap introduced by finite beta effects. The latter is sometimes indicated as the low frequency gap; we avoid this term since in this context low frequency means tearing mode frequency, i.e. below 20 kHz. There is a clear causal relationship between the development of large magnetic islands produced by $m_0 = -2$, $n_0 = -1$ tearing modes and the appearance of HF waves in FTU; in fact the latter only appear above a threshold island amplitude, as discussed in section 2. The observation of HF waves in ohmic plasmas, where high-energy ions are absent, calls for the identification

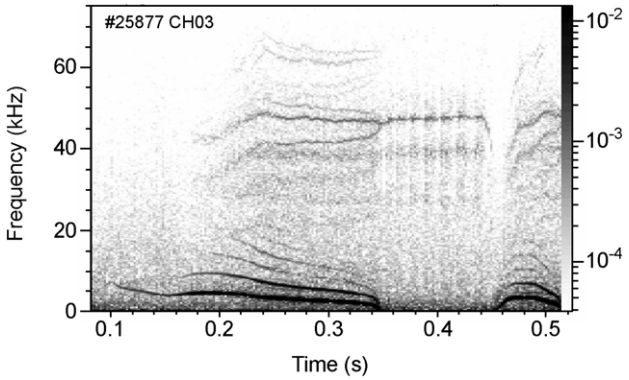

Figure 1. Spectrogram of poloidal magnetic field oscillations from a Mirnov coil at 11° above the midplane in FTU ohmic pulse 25877 with $B = 5.9\,\mathrm{T}$, $I_\mathrm{p} = 0.49\,\mathrm{MA}$, $\bar{n}_\mathrm{e} = 0.4 \times 10^{20}\,\mathrm{m}^{-3}$. The current flat top starts at $t = 0.15\,\mathrm{s}$. Greyscale indicates the relative amplitude of poloidal field oscillations $\delta B_\mathrm{pol}/B_\mathrm{pol}$. Lines below 20 kHz correspond to a $(-2, -1)$ tearing mode and its 'temporal' harmonics; amplitude is partly outside the greyscale upper edge. HF lines with different time evolution can be seen between 30 and 70 kHz. The intense HF line near 50 kHz has $n = -1$; the other just below has $n = 1$. Density is constant after $t = 0.15\,\mathrm{s}$, with an associated TAE frequency of 0.64 MHz. Temperature at $q = 2$ radius is 0.5 keV, corresponding to $\omega_\mathrm{BAE}/2\pi = 62\,\mathrm{kHz}$.

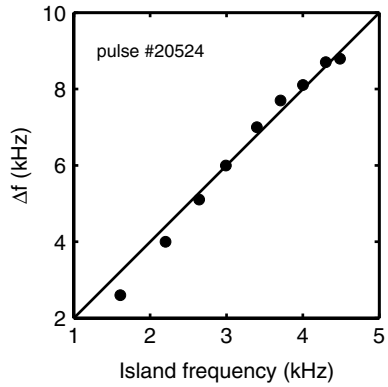

Figure 2. Frequency difference between the two dominant HF lines versus the island rotation frequency.

of a new energy source from which HF waves tap energy. Possible explanations of HF modes excitation in the presence of magnetic islands are outlined in section 3.

2. Experimental results

FTU is a compact, high field tokamak, with major radius $R_0 = 0.935\,\mathrm{m}$, minor radius $a = 0.3\,\mathrm{m}$ and maximum magnetic field $B = 8\,\mathrm{T}$. Magnetic activities are analysed by means of a set of poloidal field pick-up coils. A total of 57 coils are installed at various toroidal and poloidal positions. Only 16 channels are at present recorded by the fast data acquisition system over 1.8 s at 500 kHz with anti-aliasing. The minimum separation in poloidal angle is 5°, so that the maximum poloidal mode number that can be dealt with is 36. Similarly, the toroidal separation is 15° allowing for a maximum toroidal mode number of 12. Internal measurements on island structure and amplitude are available from soft x-ray and electron cyclotron emission (ECE) diagnostics.

HF modes were first observed in ohmic discharges with low density and edge safety factor $q_a > 5$. In these discharges magnetic islands formed by tearing instabilities around the $q = 2$ surface can saturate at large amplitudes without provoking disruptions [6], so that the development of HF modes can be studied at nearly steady-state conditions. HF modes have been recently observed in other (transient) conditions, for example, during disruption precursors.

2.1. MHD spectra

The typical frequency of magnetic oscillations produced by island rotation (island frequency in short) is 5 kHz when the island is relatively small (poloidal field fluctuations at the edge $\delta B_\mathrm{pol}/B_\mathrm{pol} < 1\%$) and decreases to zero if the island grows further. MHD spectrograms show several harmonics of low frequency oscillations extending up to 20 kHz at most (figure 1). Mode analysis at the fundamental frequency gives poloidal number $m_0 = -2$ and toroidal number $n_0 = -1$, where negative mode numbers indicate propagation in the electron diamagnetic drift direction. The '0' subscript is used to identify the tearing mode, while numbers without subscript are used in the following for HF modes. Higher harmonics may be due either to the presence of higher spatial harmonics in the island structure, or to non-uniform rotation ('temporal' harmonics). In the discharge shown in figure 1 the island appears at $t = 0.1\,\mathrm{s}$, during current rise; its amplitude progressively grows and harmonics of the 'temporal' type appear. During the interval $0.35 < t < 0.45\,\mathrm{s}$ the island disappears from the spectrogram because its frequency is below the bandwidth of magnetic coils; ECE and soft x-ray diagnostics show that during this interval the island frequency decreases from 100 to 60 Hz at constant amplitude (half-width $w \approx 2\,\mathrm{cm}$). At $t = 0.45\,\mathrm{s}$ there is an internal disruption, the island amplitude drops and a new cycle of island growth starts.

HF oscillations appear at $t = 0.18\,\mathrm{s}$; several lines can be distinguished between 30 and 70 kHz (figure 1). The two most intense lines have maximum amplitude $\delta B^\mathrm{HF}_\mathrm{pol}/B_\mathrm{pol} \approx 5 \times 10^{-4}$. The frequency difference between the two main HF lines is exactly twice the fundamental frequency of island oscillations (figure 2). As the island amplitude grows, its frequency decreases and the two lines merge; this happens at $t = 0.35\mathrm{s}$ in figure 1.

2.2. Spatial structure of high-frequency modes

Mode analysis of the two dominant HF lines gives $n = 1$ (i.e. counter-rotation with respect to the island) for the lower frequency line and $n = -1$ (i.e. co-rotation) for the higher frequency line. This implies that, if the ratio between poloidal and toroidal velocities is the same for all modes, the observed frequency difference can be accounted for by the Doppler shift due to island rotation; it follows that the two HF modes propagate at exactly opposite velocities (and then form a standing wave) in the island rest frame. A standing wave structure can indeed be observed in the amplitude of magnetic signals when the island rotates at very low frequency (figure 3). The trace in figure 3(*b*) shows temperature oscillations associated with island rotation. If island wavevector and velocity are $\boldsymbol{k}_0$ and $\boldsymbol{v}_0$, respectively,

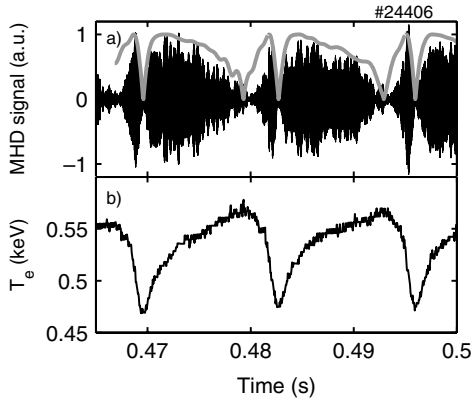

Figure 3. (*a*) HF signals (filtered with 42–53 kHz bandpass) from magnetic coil 5 (16° above midplane) showing beat-waves structure. (*b*) Temperature oscillations from an ECE channel ($R = 0.8$ m) close to the island position, showing (non-uniform) island rotation. The grey trace in (*a*) shows the envelope as expected from the phase of signal (*b*).

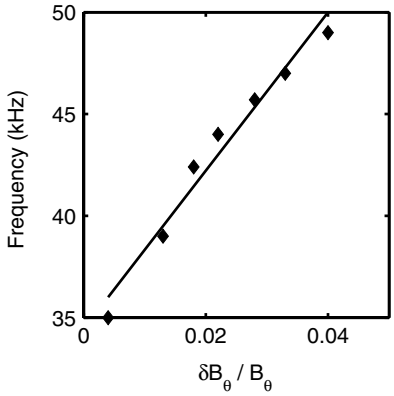

Figure 4. Frequency of the $n = -1$ HF mode as a function of tearing mode oscillation amplitude; the latter is proportional to the squared island width.

the temperature modulation is proportional to $\cos\phi_0$, where $\phi_0 = \boldsymbol{k}_0 \cdot \int \boldsymbol{v}_0 \, \mathrm{d}t$, while the superposition of two HF waves with common frequency ω (in the island rest frame) and wavenumbers $\boldsymbol{k}_1$ and $\boldsymbol{k}_2$ is proportional to $\cos(\omega t) \cdot \cos(\delta\phi + (\phi_1 - \phi_2)/2)$, where $\phi_{1,2} = \boldsymbol{k}_{1,2} \cdot \int \boldsymbol{v}_0 \, \mathrm{d}t$ and $\delta\phi$ is a constant phase shift; the latter accounts for the angular distance between temperature and magnetic diagnostic channels. Using $\delta\phi = \pi/2$ and assuming $\boldsymbol{k}_1 = -\boldsymbol{k}_2 = \boldsymbol{k}_0$, the HF signal envelope takes the form $|\sin(\phi_0)|$, which is shown by the grey curve in figure 1(*a*). For each island oscillation cycle the envelope has two minima that correspond to island O and X-points. The effect of slow island rotation can also be seen in figure 1 as periodic modulation of the spectral amplitude in the interval $0.35 < t < 0.45$ s.

The poloidal structure of HF modes from phase analysis of magnetic signals from low field side coils gives $m = 2$ for the $n = 1$ mode and $m = -2$ for the $n = -1$ mode, while $|m| > 5$ turns out from high field side coils due to toroidal effects.

2.3. HF modes dependence on island amplitude

HF modes appear if the low frequency oscillation amplitude exceeds a threshold value of 0.2%. Their frequencies increase with island amplitude, as shown in figure 4.

HF mode frequency increases by 30% while island amplitude increases by an order of magnitude; at the same time, the island frequency decreases due to electromagnetic torque originated by image currents and field errors. HF mode frequency then increases while island frequency decreases; this excludes any possibility of explaining HF modes as island deformations due, for example, to toroidal ripple—in fact, in this case, the HF mode frequency would be proportional to the island frequency.

3. Interpretation

The main experimental results presented in the previous sections can be summarized as follows: (1) HF modes only appear when a magnetic island reaches a threshold amplitude, (2) HF mode frequencies range from 30 to 70 kHz, (3) HF modes form standing-wave structures in the island rest frame and (4) HF modes are observed in ohmic plasmas in which fast ions are absent. In this section two possible interpretations will be outlined. The first one is based on the excitation of BAE modes by non-linear interaction with the island. In the second interpretation the magnetic island is considered to be a new equilibrium with very high magnetic shear near the separatrix, where kinetic Alfvén waves can develop.

3.1. Non-linear excitation of beta-induced AE

The frequency range of HF modes is inside the low frequency gap introduced in the shear-Alfvén continuous spectrum by finite beta effects [7], while the toroidicity-induced gap [8] is one order of magnitude higher (e.g. the TAE gap for the discharge in figure 1 is centred at 0.64 MHz). Since in ohmic plasmas considered in this paper there are no fast ions that can excite Alfvén modes, the observed perturbations are likely to be due to the non-linear excitation of shear-Alfvén waves by the magnetic island. More precisely, we conjecture that modes of the BAE branch [7] are nearly marginally stable in the case under investigation and can be non-linearly excited in the presence of a sufficiently large magnetic island. These modes are kinetic interchange waves, which are radially localized about their mode rational surface and are typically damped via curvature-drift Landau damping, unless the thermal ion diamagnetic frequency (temperature gradient) is sufficiently strong [3]. The lowest order BAE angular frequency can be estimated by

$$\omega_{\mathrm{BAE}} = \frac{1}{R_0}\sqrt{\frac{2T_\mathrm{i}}{m_\mathrm{i}}\left(\frac{7}{4} + \frac{T_\mathrm{e}}{T_\mathrm{i}}\right)}, \qquad (1)$$

i.e. by the accumulation point of the low frequency gap introduced in the shear-Alfvén continuous spectrum because of finite beta [3]. This frequency is an upper bound for the expected mode frequencies, consistent with experimental observations; in fact for deuterium ions with $T_\mathrm{i} = T_\mathrm{e} = 0.5$ keV we have $\omega_{\mathrm{BAE}}/2\pi = 63$ kHz. Pairs of BAEs, with given helicity and localized near the $q = 2$ surface, can interact with the $(-2, -1)$ island via three-wave couplings and be non-linearly excited provided that the energy transfer rate

from the island to BAEs is sufficient to overcome the linear mode damping, thereby setting a threshold condition for the island amplitude. For example, a $(-4, -2)$ and $(2, 1)$ BAE pair can non-linearly interact with the $(-2, -1)$ island. Note that negative mode numbers, in the present convention, correspond to modes propagating in the electron diamagnetic direction, like the tearing mode. Similar conclusions can be drawn for a $(-6, -3)$ and $(4, 2)$ BAE pair and so on, including both the positive and negative sides of the mode number spectrum.

For each BAE propagating in the electron diamagnetic direction, our model predicts that there will be a twin BAE wave propagating in the ion diamagnetic direction. These twin waves will look like standing waves in the plasma rest frame, the phase coherence being set by the common non-linear excitation mechanism, i.e. the $(-2, -1)$ island. However, as discussed above, they are not these twin waves that form the BAE pair non-linearly interacting with the tearing mode via three-wave couplings. Detailed theoretical work is underway, providing the formal analytical support for our conjecture and its benchmark against experimental results. For now, we can definitely state that our conjecture is in qualitative agreement with the observations and provides an explanation of the dominant $(2, 1)$ and $(-2, -1)$ HF modes shown in figure 1. In fact, assuming that these modes are BAEs, as discussed above, they ought to be radially localized about the $q = 2$ surface, as other non-linearly excited BAEs. Lower mode numbers, then, have higher amplitude at the plasma edge and dominate the Mirnov coil spectrum. At the lowest order, the $(2, 1)$ and $(-2, -1)$ HF modes are degenerate in the plasma frame. However, in the presence of finite plasma rotation, the $(-2, -1)$ mode accelerates while the $(2, 1)$ slows down, till mode locking sets in and mode frequency becomes degenerate once more.

3.2. High-shear effects near the island separatrix

The model presented in section 3.1 can explain the main experimental observations and it clearly indicates the energy source for an HF wave. In this section a different approach is presented, which possibly accounts for the dependence of HF mode frequency on island amplitude.

A finite-amplitude tearing mode with $m_0/n_0 = q_0$ changes the magnetic field topology by forming islands around the radius $r = r_0$, where $q(r) = q_0$ (figure 5). The key feature of the equilibrium with magnetic island is a very rapid variation of field lines pitch near the separatrix, implying a rapid variation of the parallel wavenumber of shear-Alfvén waves. The latter can be evaluated as $ik_\parallel \xi = B^{-1}\boldsymbol{B}\cdot\nabla\xi$, where ξ is any component of the wave field and $\boldsymbol{B}$ is the equilibrium magnetic field. In the unperturbed, nearly cylindrical equilibrium we have $\boldsymbol{B} = \nabla\alpha \times \nabla(\theta - \zeta/q)$, where $2\pi\alpha$, θ and ζ are toroidal flux, poloidal angle and toroidal angle, respectively; in this case, for a single-helicity wave $\xi \propto \exp(im\theta - in\zeta)$ with $m/n = q_0$, we have the obvious result $k_\parallel = m/(R_0 q_{*\mathrm{cyl}})$, where $1/q_{*\mathrm{cyl}} = 1/q - 1/q_0$. Introducing the helical angle $\beta = \theta - \zeta/q_0$, the above expressions transform to $\boldsymbol{B} = \nabla\alpha \times \nabla(\beta - \zeta/q_{*\mathrm{cyl}})$ and $\xi \propto \exp(im\beta)$. In the island-modified equilibrium the magnetic field can be expressed as [9] $\boldsymbol{B} = \nabla\alpha_* \times \nabla(\theta_* - \zeta/q_*)$, where α_* and θ_* are generalized toroidal flux and island helical angle, respectively. For field lines inside the island, q_* gives the number of rotations around the torus that a field line takes to complete one revolution around the island O-point. The parallel differential operator is $\boldsymbol{B}\cdot\nabla = J^{-1}(q_*^{-1}\partial/\partial\theta_* + \partial/\partial\zeta)$, where $J = R_0/B_0$ is the Jacobian of island coordinates. For single-helicity modes that are separable in the island flux coordinates, the parallel wavenumber is given by

$$k_\parallel = \frac{m}{(R_0 q_*)}. \tag{2}$$

If the radial scale length of the (m_0, n_0) tearing perturbation is large compared with the island width, flux contours are given by $(r - r_0)^2/w^2 = \kappa^2 - \sin^2(m_0\beta/2)$ and we have the simple expressions

$$q_* = \left(\frac{4}{\pi}\right)\left(\frac{1}{n_0 s}\right)\left(\frac{r_0}{w}\right) K(\kappa) \qquad (\kappa < 1) \tag{3}$$

and

$$q_* = \left(\frac{4}{\pi}\right)\left(\frac{1}{n_0 s}\right)\left(\frac{r_0}{w}\right)\left(\frac{1}{\kappa}\right) K\left(\frac{1}{\kappa}\right) \qquad (\kappa > 1), \tag{4}$$

where κ is a flux label chosen to have $\kappa = 0$ at the O-point and $\kappa = 1$ at the separatrix, K is the complete elliptic integral of the first kind, s is magnetic shear at r_0 and w is the island half-width. At the separatrix q_* diverges and $k_\parallel = 0$; this means that the separatrix is a rational surface for the assumed mode structure. Far from the island we have the 'cylindrical limits' $1/q_* \approx -m_0/(2q_{*\mathrm{cyl}}) \approx s n_0 (r - r_0)/2$ and $\theta_* \approx -m_0\beta/2$ (signs follow conventions in [9]). Radial profiles of $1/q_*$ along the directions $\beta = 0$ (O-point) and $\beta = \pi/2$ (X-point) are shown in figure 6 together with the cylindrical limit. The key feature of these profiles is a very steep variation near the separatrix, which is equivalent to very high magnetic shear.

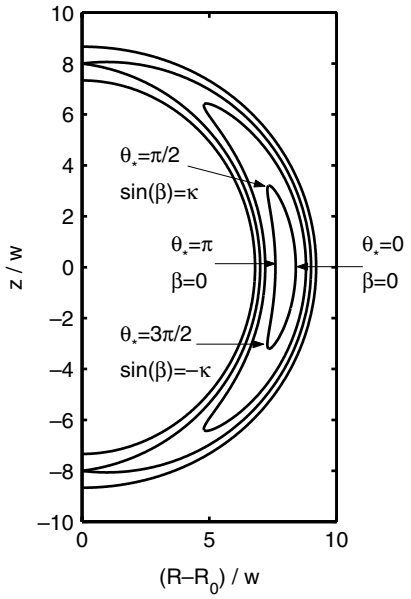

Figure 5. Schematic of $m = 2$ island flux surfaces with normalized island width $w/r_0 = 0.125$, which is representative for the conditions of figure 3, $r_0 = 16$ cm and $w = 2$ cm. Contours are shown for $\kappa = 0.4, 0.8, 1.0$ (the separatrix) and 1.2. The z coordinate represents distance from the equatorial plane.

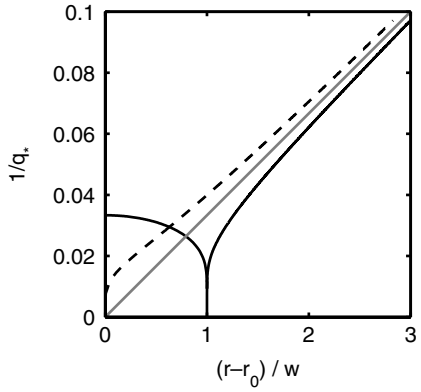

Figure 6. Radial profiles of the inverse helical q at $\beta = \pi/2$ (- - - -, separatrix at $r = r_0$) and at $\beta = 0$ (——, separatrix at $r = r_0 + w$). Profiles are calculated for $s = 1$ and $n_0 = 1$. The straight line in grey shows the no-island slope $1/q_{*\mathrm{cyl}}$.

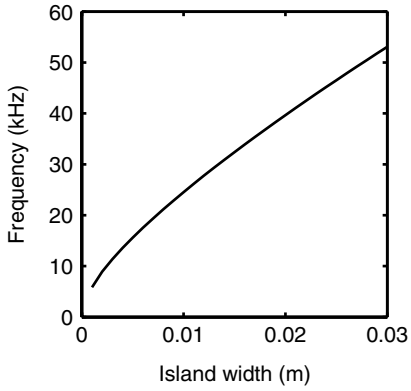

Figure 7. Frequency of discrete Alfvén modes from equation (5) as a function of island size. Plasma parameters are $V_\mathrm{A} = 1.7\times 10^7\,\mathrm{m\,s^{-1}}$, $d_\mathrm{e} = 1\,\mathrm{mm}$, $\rho_\mathrm{S} = 0.77\,\mathrm{mm}$, $r_0 = 160\,\mathrm{mm}$, $\nu_\mathrm{ei} = 0.13\,\mathrm{MHz}$, $k_\perp = 2/r_0$, $q_0 = 2$, $n_0 = 1$.

The existence of a high-shear layer near a rational surface has a profound influence on the properties of kinetic Alfvén waves. In slab geometry with resistive dissipation a discrete spectrum is found with frequencies proportional to $\omega_0 = k_{\parallel\rho} V_\mathrm{A}$ [10], where $k_{\parallel\rho}$ is the parallel wavenumber at distance ρ_S (the ion-sound Larmor radius) from the rational surface. Detailed calculations including ion response [11] give

$$\omega = \frac{2n\pi\omega_0}{\ln(\omega/(\nu_\mathrm{ei} d_\mathrm{e}^2 k_\perp^2))}, \tag{5}$$

where ν_ei and d_e are the collision frequency and the collisionless skin depth, respectively. Figure 7 shows $\omega/2\pi$ evaluated at distance ρ_S from the separatrix along the $\beta = \pi/2$ direction. Although the slab model with constant shear is a very crude estimate for the separatrix region, the estimated frequencies are in qualitative agreement both with measured frequencies and with their dependence on the island width.

This line of interpretation is less promising than the one presented in section 3.1; in particular, it is not able to explain the phase coherence between twin waves; however, the geometric features pointed out in this section are potentially useful for the development of a complete theory.

4. Conclusions

The main conclusion of this work is that the development of magnetic islands can open new channels of instability to AEs. The observed HF modes saturate at very small amplitudes in ohmic plasmas, where energetic ions are absent, but they could become a new loss mechanism in the presence of fusion-generated alpha particles. HF modes observed in ohmic plasmas near the boundary of the beta-induced Alfvénic gap have been interpreted as BAEs that are non-linearly excited via three-wave coupling with a sufficiently large magnetic island. The possibility that the helical equilibria formed by the island development become unstable to shear-Alfvén waves has also been considered. Further analysis of HF waves will be pursued by collecting a database from different tokamaks with a wide span of relevant frequencies; useful data for such a database have recently been obtained at TEXTOR [12]. Frequency scaling will give the experimental constraints for the development of a complete theory.

References

[1] Turnbull A.D. *et al* 1993 *Phys. Fluids* **B5** 2546
[2] Heidbrink W.W. *et al* 1993 *Phys. Rev. Lett.* **71** 855
[3] Zonca F. *et al* 1996 *Plasma Phys. Control. Fusion* **38** 2011
[4] Zonca F. *et al* 1999 *Phys. Plasmas* **6** 1917
[5] Sharapov S E *et al* 2004 *Proc. 20th Int. Conf. on Fusion energy 2004 (Vilamoura,2004)* (Vienna: IAEA) CD-ROM file EX/5-2Ra and http://www.naweb.iaea.org/napc/physics/fec/fec2004/datasets/index.html
[6] Buratti P. *et al* 1997 *Plasma Phys. Control. Fusion* **39** B383
[7] Chu M.S. *et al* 1992 *Phys. Fluids* B **4** 3713
[8] Kieras C.E. and Tataronis J.A. 1982 *J. Plasma Phys.* **28** 395
[9] Swartz K. and Hazeltine R.D. 1984 *Phys. Fluids* **27** 2043
[10] Catto P.J., Rosenbluth M.N. and Tsang K.T. 1979 *Phys. Fluids* **22** 1284
[11] Connor J.W., Tang W.M. and Taylor J.B. 1983 *Phys. Fluids* **26** 158
[12] Zimmermann O. *et al* 2005 *Proc. 32nd EPS Conf. on Plasma Physics (Tarragona, Spain, 27 June–1 July 2005)* P4.059